SIMMER modelling of accident initiation phase in sodium fast reactors

Xue-Nong Chen *, Andrei Rineiski

Institute for Neutron Physics and Reactor Technology, Karlsruhe Institute of Technology, Karlsruhe, Germany

A B S T R A C T

The SIMMER-III code was developed mainly for simulation of hypothetical reactor accidents after core melting, but can be applied also for accident initiation phase simulations in sodium and other liquid–metal-cooled fast reactors. New thermal hydraulic and neutronic simulation approaches and models have been developed for treatment of the initiation phase. Two examples of simulation of unprotected loss of coolant flow (ULOF) transients, in ESFR-SMART and FFTF reactors, are presented. It can be concluded that the SIMMER code has a large potential for application to initiation phase analyses.

1. Introduction

The SIMMER code (SIMMER-III and SIMMER-IV) includes advanced fluid-dynamics/multiphase-flow and neutronics models (Kondo et al. 1992, Yamano et al. 2008). The code is applied for simulation of hypothetical severe accidents in sodium fast reactors (SFRs) and other systems, e.g. accelerator driven systems with lead–bismuth eutectic (LBE) or lead cooling (Suzuki et al. 2005, Wang et al. 2008), with focus on core behaviour after core melting. An accident initiation phase (IP) of a severe accident in SFR, before can-wall melting onset, can usually be simulated with a different code; this may facilitate IP analyses but may introduce uncertainties related to coupling of SIMMER with this different code at the end of IP. We have developed several new simulation approaches and models for SIMMER recently in order to facilitate its application to IP. The following thermal hydraulic simulation approaches have been applied and tested at KIT:

- Treatment of coolant in inter-subassembly gaps, for which special meshes in plane are allocated,
- Sub-channel-scale mesh modelling,
- Heat exchanger modelling with boundary conditions for the secondary circuit coolant, instead of a simpler approach for heat sink in the primary circuit
- Gas-Expansion Module (GEM) treatment.

Moreover, the new neutronic models have been developed and tested in KIT for taking into account:

- Reactivity feedbacks due to thermal core expansion in axial and radial directions,
- Control rod driveline (CRDL) expansion reactivity feedback.

As examples of application of some of abovementioned models, we show in the following our recent transient simulation results, in particular for unprotected loss of coolant flow (ULOF) in ESFR-SMART (Mikityuk et al., 2017) and for the loss of flow without scram (LOF-WOS) test in the Fast Flux Test Facility (FFTF) (Sumner et al., 2018) with emphasis of Gas Expansion Module (GEM) direct simulation in the FFTF case. The former case (ESFR-SMART) comes from an EU-Project on a large sodium-cooled reactor design, where ULOF transient was investigated as a benchmark. The latter one is a benchmark that was organized as an IAEA collaborative research project (CRP), including a blind phase and a second phase, during which the models can be improved using experimental results. The GEM and Doppler feedback effects are two dominant ones in FFTF, which are negative and positive during the transient, respectively. The flow rate, net reactivity and power variations are simulated quite accurately with the improved GEM model. As for the GEM modelling, we focus in the following on calculations of the sodium level in GEM and related reactivity feedbacks.

2. SIMMER application to ESFR-SMART studies

The first SIMMER application example in this paper is simulation of a ULOF transient in ESFR-SMART. The power, reactivity and the mass flow rate are well predicted, while the two new abovementioned reactivity feedback models are applied in reactivity computations, in addition to standard SIMMER ones that take variations of the sodium density, fuel temperature, etc into account. SIMMER simulation model and results were presented in (Chen et al. 2022, 2023). There is a particular phenomenon found in the numerical simulations, namely,

* Corresponding author.
E-mail address: xue-nong.chen@kit.edu (X.-N. Chen).

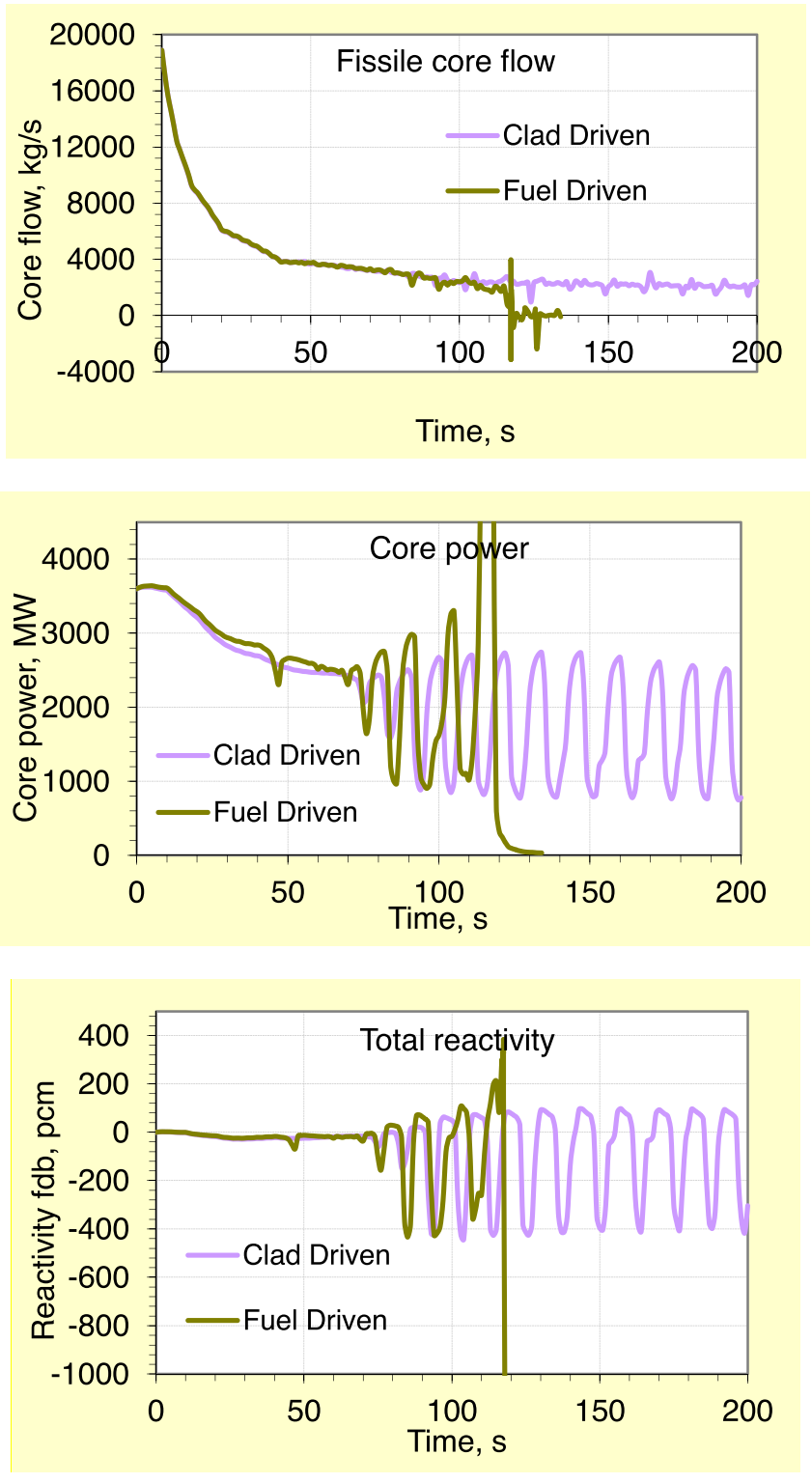

Fig. 1. ULOF results of mass flow rate, power and total reactivity in clad driven and fuel driven axial thermal expansion cases.

sodium-boiling-induced power oscillations. They are discussed in detail in (Chen et al. 2023).

In this paper we choose two typical modelling cases and show the main results. In the first case we assume that the fuel-clad gaps in all fuel pins are closed due to a relatively high fuel burn-up, therefore the axial fuel thermal expansion is driven by the clad thermal expansion, i.e. depends on the clad temperature (Clad Driven). In the second case we assume that all fuel gaps are open, which is usually observed for a fresh or low burn-up fuel, therefore axial fuel thermal expansion depends on the fuel temperature (Fuel Driven). Note that the fuel- and clad-driven axial thermal expansion effects give reactivity variations of different signs: the fuel-driven one is positive under considered conditions, as the fuel temperature decreases during the transient, while the clad-driven one is negative, as the clad temperature increases. Fig. 1 shows the results for these two cases. The "Fuel Driven" case results in a power excursion and core degradation, where the maximum reactivity is

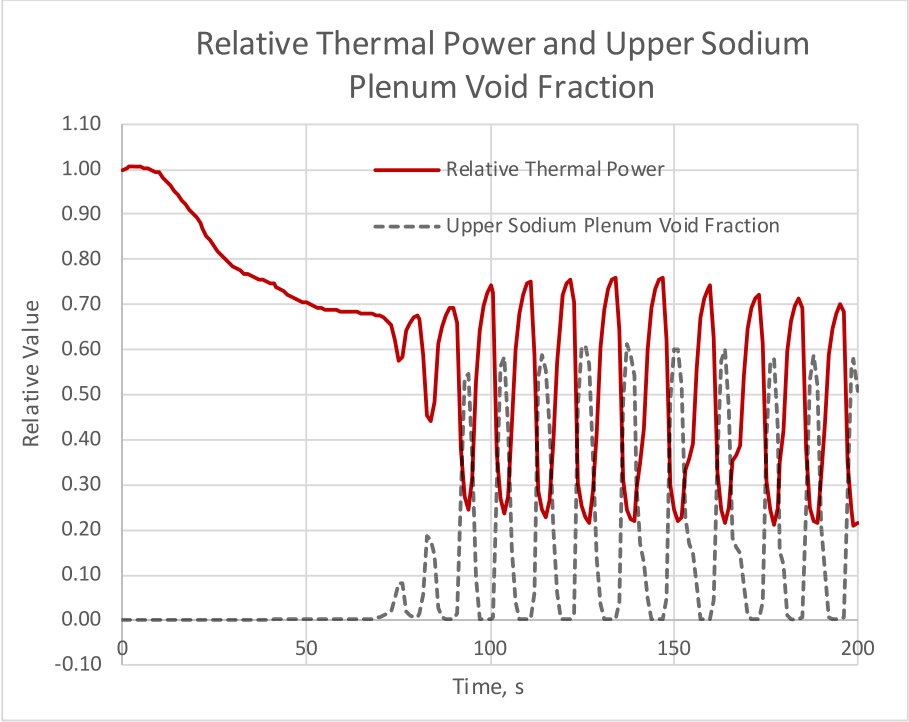

Fig. 2. Relative core thermal power and upper sodium plenum void fraction.

slightly over 1 $ during the transient, while the "Clad Driven" case also leads to sodium boiling, but gives no strong power excursion, the reactivity is positive at some times, but remains always below 1 $ during its oscillation. This is in line with earlier studies showing that the sodium boiling can lead to a power excursion, if the negative reactivity feedback is not strong enough.

In both cases in Fig. 1 we see power and reactivity oscillations after the sodium boiling on-set. We want to explain this phenomenon with Fig. 2 in the "Clad Driven" case. ESFR-SMART design includes a so-called sodium plenum above the core, with only sodium inside can-walls. The sodium void effect is positive in the core, except core boundaries, but negative in the plenum and a small region below the plenum. During the transient, as the sodium boiling takes place in the upper sodium plenum, the negative sodium density/void feedback reduces the power, and then, as the power decreases, the sodium liquid comes back to the void region, which gives a positive reactivity feedback, and then the power increases again. Fig. 2 shows the relative power and the void fraction in the upper sodium plenum. It can been seen that the power and sodium void are anti-phased, i.e. the power troughs and peaks correspond to sodium void and re-flooding states. That gives directly the reason for the oscillation, that the sodium boiling and re-flooding in the upper coolant plenum induce negative and

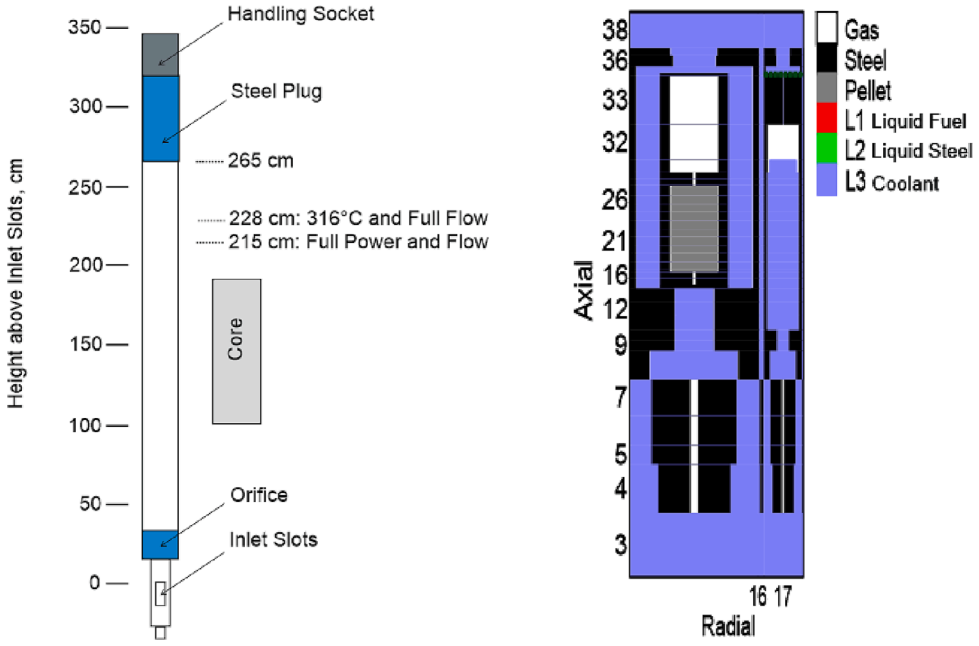

Fig. 3. GEM design plant conditions and sodium levels (left) and SIMMER 2-D GEM model (right).

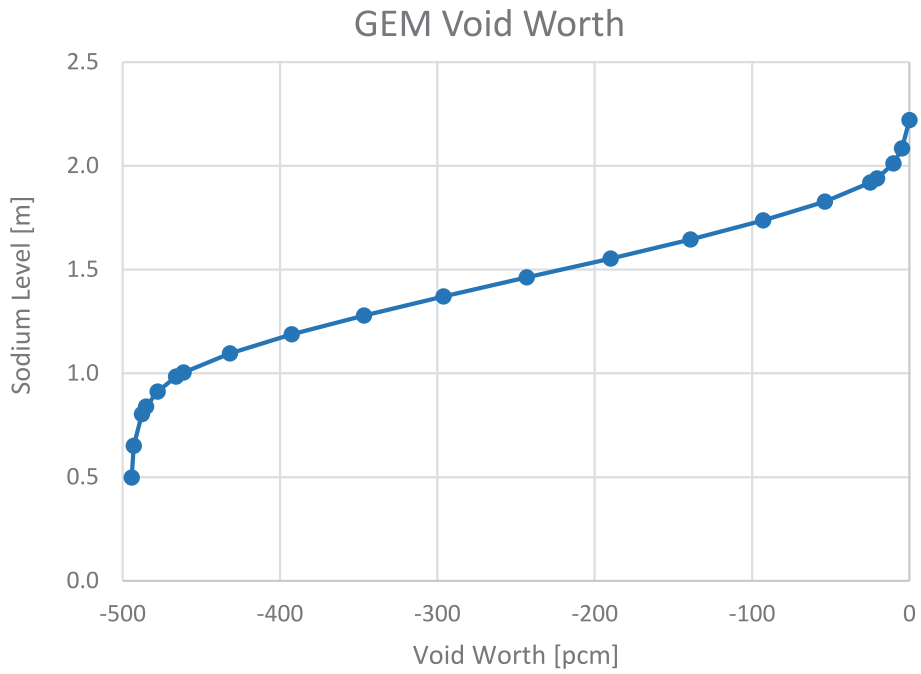

Fig. 4. Sodium level vs. calculated void worth, where the sodium level origin is the top of inlet flow holes.

positive reactivity variations, and then the power decreases and increases, respectively. These phenomena repeat with a period of about 10 s. This is influenced in particular by times for the heat transfer from fuel pellets through the gap and clad to coolant and for the heat transfer due to coolant convection from the core to the upper sodium plenum. This time shift/delay in heat transfer from fuel to the coolant in the negative sodium void effect domain is an essential reason for the periodic bifurcation during the transient, namely, Hopf bifurcation.

3. SIMMER application to FFTF studies

The second SIMMER application example is the FFTF LOFWOS transient simulation. Gas Expansion Modules (GEMs) are a key instrument in FFTF for mitigation of consequences of unprotected loss of coolant flow transients. In total 9 GEMs are inserted as subassemblies in the innermost ring of the radial reflector region. A certain volume of Argon gas is trapped by a plug at the top of each module and exposed to sodium at the bottom of the module (Sumner et al., 2018).

At nominal full flow conditions, the pressure in the sodium domain is high enough to keep the gas compressed, and the sodium-gas interface

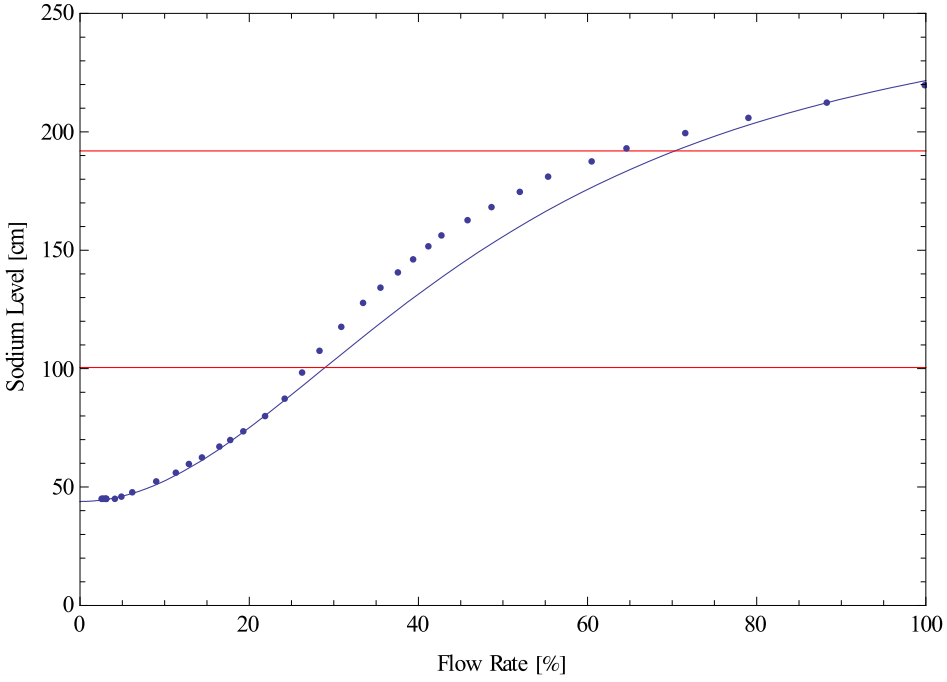

Fig. 5. SIMMER calculated GEM sodium level vs. relative flow rate during the ULOF transient in FFTF, where dots stand for SIMMER results and the curve for theoretic prediction (Sumner et al., 2018).

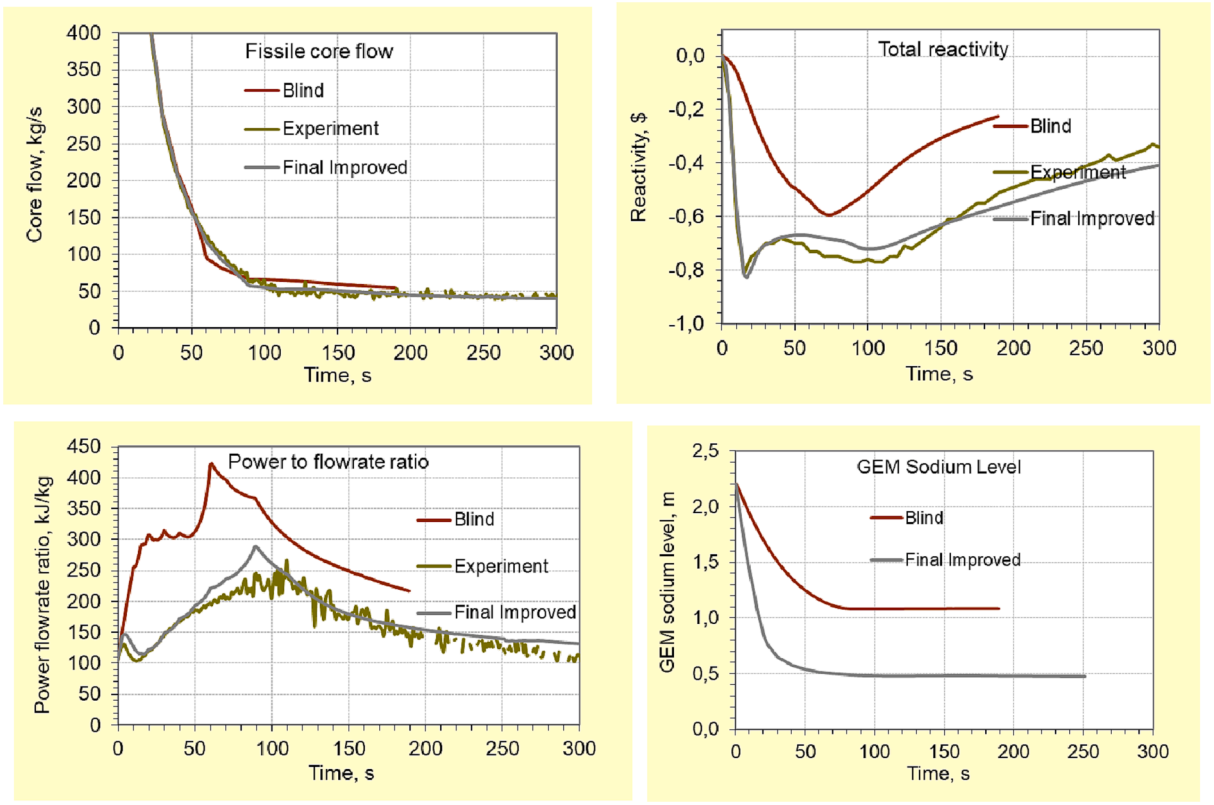

Fig. 6. Results of core mass flow rate, total reactivity, power to flow rate ration and GEM sodium level during the LOFWOS transient in FFTF.

level is above the top of the active fuel column. The exact sodium level within each GEM depends on the inlet sodium pressure, which is a function of the primary system flow rate and gas temperature, both affected by the reactor power level and core inlet temperature. During a loss of flow transient, the pressure exerted on the gas by the sodium decreases, allowing the gas to expand. At low flow rates, the sodium-gas interface level within each GEM is below the bottom of the fuel column. The displaced sodium at the core periphery leads to an increased neutron leakage and a corresponding negative reactivity feedback (Sumner et al., 2018).

Since SIMMER is a coupled code including a multiphase Advanced Fluid Dynamics Model and a neutron transport solver, reactivity feedbacks due to variation of the sodium-gas interface level in GEMs affecting the neutron leakage from the core can be directly simulated by SIMMER for LOFWOS transients. Practically, since we apply SIMMER-III, using an approximate 2-dimentional R-Z model, we should allow some simplifications and modifications. Two main aspects should be properly addressed in the modelling. One is the neutron leakage through the GEM voided region and the other one is the GEM sodium level varying with the pump driving pressure. Fig. 3 illustrates the SIMMER 2-D GEM model, where L3 stands for liquid sodium, L1, L2, L4 and other components are not present at close to nominal conditions. The GEM void worth, as calculated with SIMMER. is 448 pcm, which is comparable to the reference value of 442 pcm provided by ANL (Sumner et al., 2020). This shows that the SIMMER GEM model is reasonable with respect to the GEM reactivity feedback. Fig. 4 shows the calculated with SIMMER GEM void worth as function of the sodium-gas interface level, where the core bottom and top are at the level of 1.0048 m and 1.9192 m, respectively, for the vertical axis with the top of the inlet flow holes as the axis origin. Fig. 5 shows the calculated with SIMMER GEM sodium level depending on the flow rate, the level computed in the open phase being compared to the theoretical prediction recommended by ANL (Sumner et al., 2018). The calculated GEM level agrees well with the theoretical predictions at the beginning and end of the LOF transient, but shows a visible discrepancy during the transient. Two effects are the possible reasons for the discrepancy: one is the temperature change in the GEM gas, which was assumed to be constant in the theoretical prediction; the other is the dynamics pressure loss, which was not taken into account in the theoretical prediction.

There were so-called “blind” and “open” phases in the coordinated research project, where the participants did not and did know the FFTF experimental results, respectively. After comparing our simulation results of the blind phase with the experimental ones, we recognised deficits in our modelling and then improved the following issues for the open phase:

- a very large GEM inlet orifice coefficient was removed;
- the delayed neutron fraction, beta-eff, was reduced to 0.00313 from 0.00364;
- GEM initial void heights were corrected;
- a radial thermal expansion model was included;
- a pressure coast down curve was slightly improved;
- the intermediate heat exchanger inlet temperature (secondary side) was changed from 297 °C to 310 °C.

Nevertheless the reactivity effects of the fuel axial expansion and control rod driveline (CRDL) expansion are still not taken into account in the open phase, because they are relatively small, which could be within the uncertainty margin of fuel and coolant feedbacks, and moreover they are of different signs (positive and negative) and partially compensate each other during the transient.

The results of blind and improved simulations together with the available experimental ones are shown in Fig. 6. The improved and experimental ones are quite similar. The large discrepancy for the blind phase results is mainly due to the GEM modelling, where a very large orifice coefficient, that resists the coolant flow, was set in the GEM inlet initially. This coefficient has been removed in the improved simulation. Unfortunately, no experimental results for GEM sodium level variations

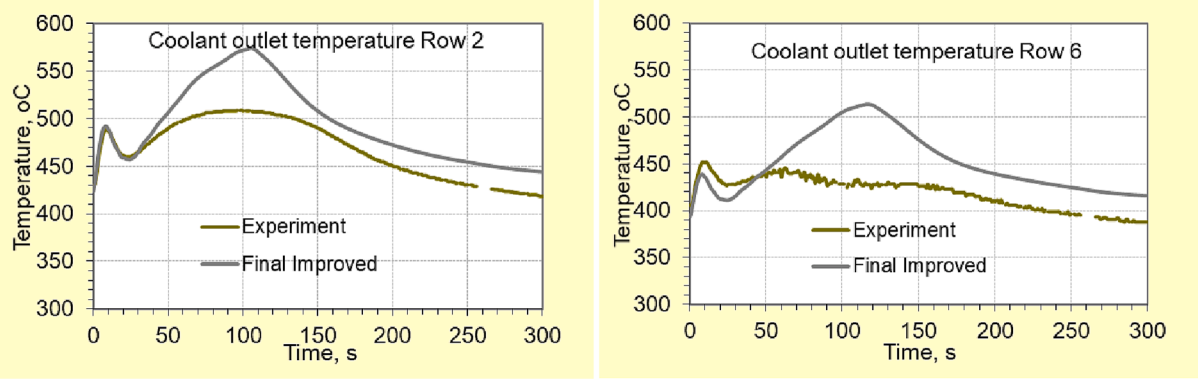

Fig. 7. Results of coolant outlet temperatures at PIOTA Row 2 and 6 during the LOFWOS transient in FFTF.

are available to compare with the calculation results shown in Fig. 6.

Fig. 7 shows the final improved results for the coolant outlet temperatures in comparison with measurements for experimental devices, PIOTA 2 and 6. In the numerical results we show average values for fuel subassembly rings. Numerical results agree very well for the first peak and trough, but not so well for the second peak. The reason is a significant discrepancy between numerical and experimental results in the power to flowrate ratio around 90 s. It is to notice that the second temperature peak at PIOTA 6 even does not appear. That may happen due to a certain reason. The neutron leakage increase due to GEM voiding during the transient leads to another effect, namely, a radial power shape variation, which may influence the PIOTA 6 outlet temperature. Since we use a 2D simulation model with one radial mesh per ring of fuel subassemblies, we can evaluate only average power variations for rings of fuel subassemblies. According to our calculations, the ratio of the power in fuel subassembly ring 6 to that in ring 2 decreases by 3% during the LOFWOS transient. In the reality, since PIOTA 6 is directly neighbouring to one of GEMs, this power shape variation at the PIOTA 6 location is expected to be much larger.

4. Conclusion

This paper summaries new SIMMER thermal hydraulic and neutronic simulation approaches and models developed at KIT for the initiation phase. Two numerical ULOF transient examples for ESFR-SMART and FFTF reactors are presented here. For the ESFR-SMART ULOF example, sodium boiling induced power oscillations have been found and explained. For the FFTF one, the simulation results are compared with experimental ones and the agreement is quite good. It can be concluded that the SIMMER code has a large potential for application to initiation phase analyses in sodium-cooled and other liquid–metal-cooled fast reactors.

CRediT authorship contribution statement

Xue-Nong Chen: Data curation, Visualization, Writing – original draft, Writing – review & editing. **Andrei Rineiski:** Visualization, Writing – original draft, Writing – review & editing, Project administration.

Declaration of Competing Interest

The authors declare that they have no known competing financial interests or personal relationships that could have appeared to influence the work reported in this paper.

Data availability

The authors do not have permission to share data.

Acknowledgements

The ESFR-SMART research leading to these results has received funding from the EURATOM research and training programme 2014-2018 under grant agreement No 754501. The FFTF data and information presented in the paper are part of an ongoing IAEA coordinated research project on “Benchmark Analysis of Fast Flux Test Facility (FFTF) Loss of Flow Without Scram Test – CRP-I32011”.

References

Chen, X.-N., Rineiski, A., Perez-Martin, S., Bubelis, E., Flad, M., 2022. “Simulations of ULOF initiation phase in ESFR-SMART with SIMMER-III”. International Conference on Fast Reactors and Related Fuel Cycles: Sustainable Clean Energy for the Future (FR22), 19-22 April 2022, IAEA, Vienna, Austria. Paper IAEA-CN-291-295.

Chen, X.-N., Rineiski, A., Perez-Martin, S., Bubelis, E., Flad, M., 2023. Numerical studies of power oscillations induced by sodium boiling in ESFR after ULOF transient. Ann. Nucl. Energy 183.

Kondo, S., Tobita, Y., Morita, K., Shirakawa, N., 1992. “SIMMER-III: An advanced computer program for LMFBR severe accident analysis”, Proceedings of the International Conference on Design and Safety of Advanced Nuclear Power Plant (ANP’92), Vol. IV, Tokyo, Japan, 1992, pp.40.5-1 to 40.5-11. Also JAEA, “SIMMER-III: A Computer Program for LMFR Core Disruptive Accident Analysis”, JNC TN9400 2003-071 (2003).

Mikityuk, K., et al., 2017. “ESFR-SMART: new Horizon-2020 project on SFR safety”, International Conference on Fast Reactors and Related Fuel Cycles: Next Generation Nuclear Systems for Sustainable Development (FR17), 26-29 June 2017, Yekaterinburg, Russian Federation. Paper IAEA-CN-245-450.

Sumner, T., et al., 2018. Benchmark specification for FFTF LOFWOS Test #13 IAEA CRP-I32011, ANL-ART-102-Rev. 2, Argonne National Laboratory, USA.

Sumner, T., et al., 2020. “LOFWOS Test #13 Measured Data and Collective Blind Phase Results”, IAEA CRP-I32011. Argonne National Laboratory, USA.

Suzuki, T., Chen, X.-N., Rineiski, A., Maschek, W., 2005. Transient analyses for accelerator driven system PDS-XADS using the extended SIMMER-III code. Nucl. Eng. Des. 235 (24), 2594–2611.

Wang, S., Flad, M., Maschek, W., Agostini, P., Pellini, D., Bandini, G., Suzuki, T., Morita, K., 2008. Evaluation of a steam generator tube rupture accident in an accelerator driven system with lead cooling. Prog. Nucl. Energy 50 (2-6), 363–369.

Yamano, H., Fujita, S., Tobita, Y., Sato, I., Niwa, H., 2008. Development of a three dimensional CDA analysis code: SIMMER-IV and its first application to reactor case. Nucl. Eng. Des. 238 (1), 66–73.